Soft Matter

Accepted Manuscript

ROYAL SOCIETY OF CHEMISTRY

www.rsc.org/softmatter

Dynamic photoinduced realignment processes in photoresponsive block copolymer films: Effects of chain length and block copolymer architecture

Masami Sano,[a] Feng Shan,[b] Mitsuo Hara,[a] Shusaku Nagano,*[c] Yuya Shinohara,[d] Yoshiyuki Amemiya,[d] and Takahiro Seki*[a]

[a] Department of Molecular Design and Engineering, Graduate School of Engineering, Nagoya University, Furo-cho, Chikusa, Nagoya 464-8603, Japan

[b] School of Chemistry and Chemical Engineering, Shanghai Jiao Tong, University, Shanghai 200240, P.R. China

[c] Nagoya University Venture Business Laboratory, Nagoya University, Furo-cho, Chikusa, Nagoya 464-8603, Japan

[d] Graduate School of Frontier Sciences, The University of Tokyo, 5-1-5, Kashiwanoha, Kashiwa 227-8561, Japan

Abstract

A series of block copolymers composed of an amorphous poly(butyl methacrylate) (PBMA) block connected with an azobenzene (Az)-containing liquid crystalline (PAz) block were synthesized changing the chain length and polymer architecture. With these block copolymer films, the dynamic realignment process of microphase separated (MPS) cylinder arrays of PBMA in the PAz matrix induced by irradiation with linearly polarized light was studied by UV-visible absorption spectroscopy, and time-resolved grazing

incidence small angle X-ray scattering (GI-SAXS) measurements using a synchrotron beam. Unexpectedly, the change in chain length hardly affected the realignment rate. In contrast, the architecture of AB-type diblock or ABA-type triblock essentially altered the realignment feature. The strongly cooperative motion with an induction period before realignment was characteristic only for the diblock copolymer series, and the LPL-induced alignment change immediately started for triblock copolymers and a PAz homopolymer. Additionally, a marked acceleration in the photoinduced dynamic motions was unveiled in comparison with a thermal randomaization process.

1. Introduction

The photoalignment has been recognized as a versatile method for orienting liquid crystalline (LC) materials.[1–6] Among many photoalignment systems, block copolymers that form periodical mircophase separation (MPS) structures have recently become attractive targets in light of facile on-demand alignment control of mesoscopic level structures ranging typically 10 – 100 nm.[7–10] In the photoprocess, the pre-aligned state by initial linearly polarized light (LPL) can be "realigned" by successive LPL with the electric vector *E* in a different direction.[1–4,11–13] The ability of realignment is expected to provide new possibilities in block copolymer nanotechnologies.[14–17]

Regarding the mechanism of photoinduced alternations of MPS structure, we have attempted to made in-situ observations of the dynamic alignment changes in thin films of diblock copolymer consisting of poly(butyl methachrylate)-*block*-azobenzene (Az)-containing LC polymer (PBMA-*b*-PAz).[18,19] This approach revealed a strongly cooperative interplay between the different hierarchical structures of the MPS cylinder pattern and smectic LC layer.[18] By capturing the intermediate state of the realignment

process by transmission electron microscopy (TEM) and polarized optical microscopy (POM), and in-situ synchrotron grazing angle X-ray scattering (GI-SAXS) measurements, the realignment was found to undergo via sub-domain rotation mechanism retaining the hierarchical structure.[19] Additional efforts using a homologous diblock copolymer possessing poly(hexyl methacrylate) (PHMA-*b*-PAz) provided precise and in-depth understandings for this dynamic process.[20]

<Scheme 1>

Although substantial knowledge has been accumulated as above, the factors of the polymer structures influencing the realignment behavior as followings still remain unrevealed. i) Influence of the chain length (molecular mass): If the rotation of the domain is the alignment mechanism, the molecular mass should affect the rate of alignment change. And ii) Influence of the block copolymer architecture: No comparative study has been achieved with diblock and triblock copolymers. In this context, we conducted a systematic investigation in this work on the photoinduced realignment process using a series of $PBMA_n$-*b*-PAz_m diblock and PAz_n-*b*-$PBMA_m$-*b*-PAz_n triblock copolymers with varied chain length (see Scheme 1). As the control, a PAz homoplymer without the MPS structure was also investigated. Additionally, regarding the realignment rate, the relaxation process (randomization of a mono-aligned state) was evaluated with and without non-polarized light exposure. A marked acceleration in the relaxation process was observed under the light exposure.

2. Results and discussions

2.1. Synthesis and characterizations of di- and tri-block copolymers

The Az-containing methacrylate monomer and polymerization procedures via atom

transfer radical polymerization (ATRP) for the di-block copolymers ($PBMA_m$-*b*-PAz_n) were synthesized according to the procedures reported in the previous paper.[18,21] The tri-block copolymers, PAz_n-*b*-$PBMA_m$-*b*-PAz_n, were synthesized in the same manners starting from a dual halogen-terminated ATRP initiator of ethylene bis(2-bromoisobutyrate).[22]

<Table 1>

Table 1 summarizes the weight-averaged molecular weight (M_W), poly dispersity index (PDI), estimated volume fractions, and number of repeating units for di- and tri-block copolymers, and a homopolymer synthesized in this work. According to the volume fractions estimated from the repeating units for PBMA and PAz by ^{1}H-NMR, all the block copolymers were expected to form a PBMA cylinder structure of PBMA in the PAz matrix. Differential scanning calorimetry (DSC) measurements showed that the thermophysical properties of PAz homopolymer and block copolymers were essentially the same exhibiting glass–55 °C–smectic A–90 °C–smectic C–118 °C–isotropic. This fact indicates that, for the block copolymers, PBMA and PAz LC blocks were phase-separated. The heat capacity change due to T_g of PBMA at 20 °C was not satisfactorily detected because of the low volume fraction of the PBMA block ranging 0.2 – 0.3. In small-angle X-ray scattering measurements (SAXS) in the bulk state, the first ordered scattering peaks of these block copolymers were observed in the small angle range from a scattering vector ($q = [4\pi (\sin \theta)/\lambda]$, θ and λ being scattering angle and wavelength of X-ray, respectively) at 0.11 to 0.21 nm^{-1}. The cylinder-to-cylinder distances (d) were calculated from q, and were also shown in Table 1. d values of the scattering peaks increased with increasing the molecular mass (M_w).[23,24]

2.2. In-plane dichroism change of Az mesogen

Spincast films of the synthesized block copolymers were prepared and annealed at 130 °C for 5 min. The annealed films were irradiated with LPL at 436 nm at 95 °C (smectic A phase of PAz). After LPL irradiation, all polymer films exhibited a large dichroism in the π–π^* absorption band of Az around 335 nm, indicating that the Az mesogens were photoaligned by LPL irradiation. Significantly larger light absorption was observed in the perpendicular direction to the *E* of actinic LPL in each film. For evaluation of aligning ability of the Az mesogens, the order parameter *S* was calculated as $S = (A_{large} - A_{small})/(A_{large} + 2A_{small})$, where A_{large} and A_{small} denote the larger and smaller absorbances, respectively, at the peak of the π–π^* band in the polarized spectra after the LPL irradiation. The *S* values at the initially aligned state are shown in Table 1. *S* values ranged from 0.53 to 0.68, indicating that the Az mesogens were highly photoaligned essentially to the same extents for all polymer films.

<Fig. 1>

By irradiation with successive LPL at 436 nm in the orthogonal direction to the initial one, the Az mesogens were realigned (see Scheme 1b). Time course changes of the in-plane dichroism are shown in Figure 1. Here, the light intensity was 1 mW cm^{-2}, and thus the time in second correspond to the energy dose in mJ cm^{-2}. To evaluate the direction and alignment level of Az mesogen, dichroic ratio, $DR = (A_\perp - A_\parallel)/(A_\perp + A_\parallel)$, was calculated, where $A_\perp$ and $A_\parallel$ denote absorbances at the peak corresponding the π–π^* transition band measured with polarized light of *E* set perpendicular and parallel to that of the LPL for the realignment, respectively.[19] The negative and positive values indicate that the Az mesogens were aligned to the initial and subsequent orthogonal directions, respectively. To compare the realignment behavior of Az mesogens of different polymer films, *DR* (normalized) = $DR / |DR_{ini}|$, $|DR_{ini}|$ denoting the absolute value of the initial *DR*

was calculated.

Figure 1a shows the *DR* changes with irradiation dose for the three diblock copolymer films ($PBMA_m$-*b*-PAz_n) having different chain lengths. The changes in *DR* (normalized) with LPL irradiation dose (time) exhibited sigmoidal curves with an induction period of approximately 50 s, and the inversion of *DR* occurred from 50 to 150 s. Thus, strong cooperativity was recognized in the alignment change process of the mesogens. The change was almost saturated at 150 s in all the diblock copolymer systems. Contrary to our expectation, the *DR* change behavior was hardly affected by the change in the molecular mass of $PBMA_m$-*b*-PAz_n. This will be discussed in section 2.4.

In contrast, the change in the polymer architecture, homopolymer (PAz_{70}) diblock compolymer ($PBMA_{128}$-*b*-PAz_{78}), and triblock copolymer (PAz_{68}-*b*-$PBMA_{128}$-*b*-PAz_{68}) led to significant differences (Fig. 2b). For the homopolymer and triblock copolymer did not exhibited the induction period. The *DR* value started to increase immediately after the start of LPL irradiation. At approximately 60 s of LPL irradiation, the homopolymer and triblock copolymer systems gave *DR* (normalized) approaching to zero, whereas the diblock copolymer system still retained at *DR* (normalized) = –0.8. The *DR* change finished at 150 s of LPL exposure similarly to the case of the diblock copolymer systems. The different behavior between the diblock and triblock copolymers is noteworthy, which will be discussed further in section 2.5.

<Fig. 2>

2.3. In situ synchrotron GI-SAXS measurements

The in situ synchrotron GI-SAXS measurements were carried out under LPL irradiation at a constant temperature (95 °C, smectic A phase of PAz) to investigate the photoinduced structural changes of hierarchical structures during the photoinduced realignment process

(Scheme 1b). The real time scattering changes were monitored for both the LC smectic layer (wider regions) and cylindrical MPS structure (smaller regions) in the block copolymer systems. The details of experimental procedures were described in our previous reports.[18–20] Typical 2D GI-SAXS image and 1D in-plane intensity profiles are displayed in Fig. 2. In the pre-aligned state of block copolymer films, the scattering peak was observed in the small angle region (q_y = 0.21 nm^{-1}, d = 29 nm for diblock PBMA$_{102}$-*b*-PAz$_{97}$ (a) and q_y = 0.19 nm^{-1}, d = 33 nm for triblock PAz$_{58}$-*b*-PBMA$_{89}$-*b*-PAz$_{58}$ (b), and no scattering was observed in the wider region. Here, q_y denotes the scattering vector in the in-plane direction. After the hierarchical structure was realigned by the successive LPL irradiation to the orthogonal direction, only the scattering from the LC smectic layer was observed in the wider region (q_y = 1.87 nm^{-1}, d = 3.4 nm). For the homopolymer, PAz$_{70}$, scattering peak was observed only in the wider region after the realignment.

<Fig. 3>

Figure 3 shows typical time course profiles of the scattering peak intensity due to the Az LC smectic layer structure in thin films for the diblock (PBMA$_{102}$-*b*-PAz$_{97}$) and triblock (PAz$_{58}$-*b*-PBMA$_{89}$-*b*-PAz$_{58}$) copolymers, and homopolymer PAz$_{70}$ at 95 °C. In part a, a schematic illustration for the setup is shown. The intensity decay and enhancement processes are separately plotted in parts b and c, respectively.

As shown in part b, the peak decay was almost ceased at 50 s for the diblock (circle) and triblock (square) copolymer systems. On the other hand, the decay profile for the homopolymer continued over 100 s. Probably, the existence of mesoscopic MPS structure of PBMA disturbs the packing of PAz mesogens. The experimental temperature (95 °C) is much higher than T_g of PBMA, and such enhanced segmental motions of PBMA can also accelerate the realignment dynamics.

The peak enhancement profiles are shown in part c. The scattering peak was observed for the three polymers commonly at approximately 150 s. The enhancing rate, on the other hand, was influenced by the polymer type, i. e., block copolymer or homopolymer. In this set of data, the scattering intensity enhanced faster for the homopolymer (triangle) than those for the diblock (circle) or triblock (square) copolymers. Compared with the peak decay profiles, the peak enhancement processes required much longer time over 600 s, which corresponds to the fusion of divided domains.[19]

<Fig. 4>

All of the block copolymer systems exhibited the similar time course profiles: The peak disappears at approximately 50 s and start to increase at approximately 150 s from the start of LPL irradiation. However, details in the realignment kinetics differ with each other. To compare the rate of scattering intensity change for different polymers, time periods required for the 65 % of the total change (T_{65}) were evaluated. At 65 % change, the difference in time period became most pronounced. In Fig. 4, the T_{65} (decay) and T_{65} (enhancement) are plotted against the cylinder-to-cylinder distance (d) of MPS structure in parts a and b, respectively.

As shown in part a, only T_{65} (decay) of the homopolymer was significantly larger than those of block copolymers. On the other hand, T_{65} (enhancement) in part b, some deviations were observed also between the block copolymers. T_{65} (enhancement) value became larger when the cylinder-to-cylinder distance exceeded 35 nm. The architecture of the copolymers (diblock or triblock) did not essentially affect this rate. It seems reasonable that the T_{65} (decay) is related the initial photoinduced local fluctuations of the smectic layer, therefore, it is not affected by the polymer chain length, In contrast, T_{65} (enhancement) is coupled with the polymer assembling process, which should be

dependent on the chain length. The discontinuous change in T_{65} (enhancement) around 30 – 35 nm of cylinder distance is noteworthy. We assume that the packing and thus the dynamic property of Az mesogens can be changed at this threshold distance from the MPS boundary interface (inter-material dividing surface).[25,26] However, a precise understanding is a subject of future investigation.

Unexpectedly, both values of T_{65} (decay) and T_{65} (enhancement) were not very sensitive to the chain length of the polymer. When T_{65} (decay) and T_{65} (enhancement) were compared between $PBMA_{102}$-*b*-PAz_{97} (d = 35 nm) and $PBMA_{211}$-*b*-PAz_{145} (d = 59 nm), these values were similar despite the large difference in d.

<Fig. 5>

2.4. POM observations

Figure 5 displays POM images at the intermediate state in the realignment process for the diblock copolymers (a ($PBMA_{127}$-*b*-PAz_{76}, d = 29 nm) and (b ($PBMA_{211}$-*b*-PAz_{145}, d = 59 nm)), triblock copolymer (c (PAz_{58}-*b*-$PBMA_{89}$-*b*-PAz_{58}, d = 33 nm)) and homopolymer (d, PAz_{70}) films with thickness of 250 nm. Each image was taken at the irradiation dose around 60 – 90 mJ cm^{-2} at 95 °C where DR = 0. All images indicate birefringent character and exhibited transient sub-micrometer sized LC domains.

When the images of two diblock copolymers with different chain lengths are compared, the domain size feature of the shorter chain length (a) was apparently larger than that of the longer one (b). We assume that the insensitive nature of realignment rate with polymer chain length (Fig. 1a) is related to the change in the sub-domain size in the alignment change proceeding via the sub-domain rotation mechanism. The diblock copolymer film with longer polymer chain generated smaller transient sub-domains in the realignment process. $PBMA_{127}$-*b*-PAz_{76} provided uniform domains around 1 μm sized

diameters (a), and PBMA$_{211}$-*b*-PAz$_{145}$ gave much smaller sized domains (b). The triblock copolymer systems exhibited the similar tendency. The realignment rate was hardly changed regardless of the chain length, namely, the size of MPS cylinder structure (Fig. 1a and Fig. 4). In this way, a compensation effect was recognized between the polymer chain length and size of the sub-domains in the transient state, which consequently led to the similar realignment rates.

<Fig. 6>

2.5. Difference between di- and triblock copolymer systems

Our previous investigation with a PBMA-*b*-PAz diblock copolymer demonstrated that the process can be divided into the following three stages.[19] Stage 1: The scattering intensity rapid decreases due to the photofluctuation without the direction change of Az mesogen until 50 mJ cm^{-2} light irradiation dose (induction period), Stage 2: Az mesogens and LC domain are rotating to the orthogonal position with the ordered MPS cylinders (reorientation period), and Stage 3: the reorientated domains are fusion and growth to orthogonal direction of actinic LPL polarized direction self-assembly (post-growth period). As shown here, all three diblock copolymers behaved in the same manner. In Fig. 6a, typical changes in the in-plane *DR* and time course profiles of the scattering intensity due to the smectic layer (q_y = 1.87 nm^{-1}, d = 3.4 nm) in the in-situ GI-SAXS measurements (peak decay in the initial direction and peak enhancement in the orthogonal direction) for the PBMA$_{102}$-*b*-PAz$_{97}$ film are shown as a typical example.[19]

In contrast, the triblock copolymer film showed different behavior. Part b displays the same set of plots for PAz$_{58}$-*b*-PBMA$_{89}$-*b*-PAz$_{58}$. *DR* increased immediately after the start of LPL irradiation concurrently with the decay of the X-ray scattering intensity. Here, Stages 1 and 2 observed in the diblock copolymer systems are virtually combined. As

shown in Fig. 1b, this behavior is similar to that of the PAz homopolymer.

The different feature of the realignment process in the di- and triblock copolymer systems can be ascribed to the difference in the stability of the MPS structure. It is known that stability of MPS structure depends on the block copolymer architecture, i. e., the MPS structure of ABA-block copolymers is less stable than AB block copolymers of comparable chain length.[27,28] Also in the case of triblock copolymers, both PBMA ends are connected with PAz chain, thereby, the motions of Az mesogens can be effectively coupled with the chain motions of PBMA. As the results, the LPL-induced realignment process becomes similar as that of the homopolymer without the MPS structure, thereby, no induction period will be observed.

<Fig. 7>

2.6. Photoprocess vs. thermal process

The present block copolymers quickly (essentially in ca. 2 min) alter the alignment of the MPS structure by LPL.[18-20] This can be compared with other reorientation processes of MPS structures under electric fields, which range some hundreds minutes.[29,30] To gain insight into this marked difference, time course measurements of in-situ GI-SAXS was conducted for the photo- and thermal relaxation (deterioration of the uniform alignment) processes at 95 °C using a $PBMA_{128}$-*b*-PAz_{78} film. The relaxation processes were observed with and without irradiation with *non-polarized* light at 436 nm (1 mW cm^{-2}).

Figure 7a shows the time course profiles of X-ray scattering intensity at q_y = 0.21 nm^{-1} from the MPS cylinder array due to the orientational relaxation (randomization) with (circle) and without (square) photoirradiation. The scattering intensity in the photo-relaxation process was rapidly reduced right after the light irradiation, and the intensity change ceased at 100 s at ca. 60 % intensity level of the initial one. On the other hand, in

the thermal relaxation, the intensity was slightly increased until 1000 s, and then decreased after 1000 s. Even after 6000 s, the peak intensity still gradually decreased. The peak enhancement at the early stage in the thermal relaxation should correspond to a cooperative ordering due to the liquid crystallinity. After 1000 s, prolonged thermal treatment deteriorated the uniaxial alignment due to thermally induced randomizations.

When T_{65} (decay) of the total change relaxation time was compared (Fig. 7a), these values were approximately 50 s and 3000 s, for the photo-assisted and dark relaxation processes, respectively. In this way, the light irradiation accelerated the randomization process by approximately 60-folds. This marked acceleration in the relaxation process under light irradiation can be related with the fast realignment of these block copolymer films upon LPL irradiation. Three factors can be assumed to account for the acceleration: i) Continuous configurational switching of Az unit during the irradiation (trans-to-cis and cis-to-trans photoisomerizations), local heating via the non-radiative process, and softening of the polymer film by involvement of the cis-isomers of Az.

The photoinduced relaxation behavior was also monitored at q_y = 1.87 nm^{-1} due to the smectic layer to compare the relaxation process together with the homopolymer. In Fig. 7b, T_{65} (decay) was plotted against the cylinder-to-cylinder distance in Fig. 7b). The block copolymers commonly gave a same level of T_{65} of approximately 50 s, and only the homopolymer provided a significantly longer T_{65} value of 115 s. These results agree with the scattering intensity decay observed in Stage 1 (Fig. 4a) in the LPL-induced realignment process.

3. Experimental section

3.1 Syntheses

Monomers and polymers were synthesized according the procedures described in the previous report.[18–20]

Weight-averaged molecular weight (M_W) and poly disparity index (PDI) of the synthesized polymers were determined by gel permeation chromatography (GPC, high-performance liquid chromatography system (Shodex DS-4/UV-41/RI-101) with Shodex KL-502 and 503 columns) with tetrahydrofran as eluent. The pump was operated at 0.3 mL min^{-1} and the measurement was calibrated with monodisperse polystyrene standards (Tosoh). Volume fractions of the block copolymers were estimated from ^{1}H NMR spectra spectrometer (GSX-270, JEOL) using tetramethylsilane signal as the standard signal. Measurement of thermophysical properties of the block copolymers were performed by DSC (DSC Q200 MO-DSC-UV, TA Instruments) with 2 $^{\circ}$C min^{-1} rate. XRD measurements for structural analysis of the MPS structures were performed with a NANO-Viewer X-ray diffractometer (Rigaku) detected by an imaging plate (FUJIFILM) with X-ray from Cu Kα radiation (α = 0.154 nm). The diameters of the X-ray beams were 0.3 − 0.6 mm which collimated by pinhole slits. Camera length was set at 960 mm.

3.2. Measurements

Polarized UV-visible absorption spectra of the thin films were taken on an Agilent 8453 spectrometer equipped with a polarizer in front of the samples.

POM measurements was carried out with an Olympus BX51-P equipped with an Olympus DP28 camera with the aid of a Cellscancontroller software. The films were heated and kept at 95 °C for the all measurements by using a HP82 thermostated stage (Mettler Toledo).

Time-resolved synchrotron GI-SAXS measurements were performed at the BL-6A of the KEK Photon factory in Tsukuba, Japan. A monochromated X-ray radiation source

at the wavelength λ of 0.150 nm with a beam size of approximately 250 μm × 500 μm was used. The detection was performed with X-ray CCD detectors (DECTRIS PILATUS 300K and 100K detectors for smaller and wider angle regions, respectively). The detailed procedures and analyses were described in the previous reports.[18–20] 2D GI-SAXS images were captured with X-ray incidence angles adjusted between 0.18° and 0.22°, which was slightly larger than the critical angle of the polymer films.

3.3. Photoalignment Procedures

Thin films were prepared on quartz plates by spincasting (2000 rpm) from a 2 % by weight chloroform solution. Before LPL irradiation, the film was first annealed at 130 °C (isotropic state of PAz) on a hotplate before LPL irradiation, and then the initial alignment was performed by irradiating with LPL at 95 °C (SmA state of PAz). Film thickness was evaluated by surface profiles obtained by AFM (Nanopics 2100, Seiko Instruments). The film was partly scratched by spatula and the height difference between the film surface and substrate surface was measured. The typical film thichness was ca. 200 nm. LPL irradiation at 436 nm was performed with a mercury lamp source (REX-250, Asahi Spectra) at 1 mW cm^{-2} with a 436 nm band-pass filter (Asahi Spectra).

4. Conclusions

This work elucidated the effects of chain length and architecture (di- and triblock copolymer types) on the photoinduced alignment changes of the hierarchical structures. The time course analyses of UV-vis spectroscopy and GI-SAXS measurements revealed the detailed motion behavior of both Az mesogen, smectic LC phase, and MPS cylinder structure. The polymer with larger mass produced the smaller sub-domains in the transient stage of realignment. As the result, the chain length of the polymer hardly affected the

photoinduced realignment rate. On the other hand, the block copolymer essentially influenced the process. The feature can be ascribed to a difference in the stability of the MPS structure. To date, photoinduced mechanical motions in block copolymer systems containing mesoscopic MPS structure have not been well understood yet. We believe that our approach and knowledge obtained here provide useful implications and clues in this respect.

Acknowledgements

This work was supported by a Grant-in-Aid for Scientific Research (S23225003 to TS and B25286025 to SN) and for Young Scientists (B25810117 to MH) from The Ministry of Education, Culture, Sports, Science and Technology (MEXT), Japan, the PRESTO program of Japan Science and Technology Agency to SN, and Grant-in-Aid for JSPS fellow (25-8132) from MEXT/JSPS to MS. This work was also supported in part by a Grant-in-Aid for Scientific Research on Innovative Areas "Photosynergetics" (No. 15H01084) from MEXT, Japan. The synchrotron X-ray scattering experiments were performed at BL-6A of the KEK-Photon Factory, Tsukuba (proposal No. 2012G629). FS of SJTU (Q. Lu group) joined this project in the framework of the three nation Campus Asia Program (Japan-China-Korea) student exchanging program.

Table 1 Polymers synthesized in this work.

Polymer	Unit		Φ_{LC}	M_w / 10^4	PDI	Cylinder distance / nm	Order parameter *S*
	BMA (m)	Az (n)					
$PBMA_{127}$-*b*-PAz_{76}	127	76	0.68	5.6	1.18	29	0.68
$PBMA_{102}$-*b*-PAz_{97}	102	97	0.77	6.2	1.36	35	0.66
$PBMA_{211}$-*b*-PAz_{145}	211	145	0.71	10.2	1.38	59	0.57
PAz_{68}-*b*-$PBMA_{128}$-*b*-PAz_{68}	128	68	0.79	8.6	1.42	28	0.53
PAz_{58}-*b*-$PBMA_{89}$-*b*-PAz_{58}	89	58	0.82	7.0	1.36	33	0.55
PAz_{70}	-	70	1.0	4.7	1.21	—	0.66

References

1. K. Ichimura, *Chem. Rev.*, 2000, **100**, 1847−1873.
2. O. Yaroshchuk and Y. Reznikov, *J. Mater. Chem.*, 2012, **22**, 286-300.
3. T. Seki, S. Nagano and M. Hara, *Polymer*, 2013, **54**, 6053-6072.
4. T. Seki, *Polym. J.*, 2014, **46**, 751-768.
5. J. Hoogboom, T. Rasing, A. E. Rowan and R. J. M. Nolte, *J. Mater. Chem.*, 2006, **16**, 1305.
6. N. Kawatsuki, *Chem. Lett.*, 2011, **40**, 548-554.
7. Y. Morikawa, S. Nagano, K. Watanabe, K. Kamata, T. Iyoda and T. Seki, *Adv. Mater.*, 2006, **18**, 883-886.
8. Y. Morikawa, T. Kondo, S. Nagano and T. Seki, *Chem. Mater.*, 2007, **19**, 1540-1542.
9. H. Yu, T. Iyoda and T. Ikeda, *J. Am. Chem. Soc.*, 2006, **128**, 11010-11011.
10. H. Yu, T. Kobayashi and H. Yang, *Adv. Mater.*, 2011, **23**, 3337-3344.
11. Y. Zhao and T. Ikeda, *Smart Light-Responsive Materials*, John Wiley & Sons, New Jersey, 2009.
12. T. Seki, *Bull. Chem. Soc. Jpn.*, 2007, **80**, 2084-2109.
13. J. Tomczyk, A. Sobolewska, Z. T. Nagy, D. Guillon, B. Donnio and J. Stumpe, *J Mater. Chem. C*, 2013, **1**, 924-932.
14. C. M. Bates, M. J. Maher, D. W. Janes, C. J. Ellison and C. G. Willson, *Macromolecules*, 2013, **47**, 2-12.
15. C. Park, J. Yoon and E. L. Thomas, *Polymer*, 2003, **44**, 6725-6760.
16. H.-C. Kim, S.-M. Park and W. D. Hinsberg, *Chem. Rev.*, 2010, **110**, 146–177.
17. S. B. Darling, *Prog. Polym. Sci.*, 2007, **32**, 1152-1204.

18. S. Nagano, Y. Koizuka, T. Murase, M. Sano, Y. Shinohara, Y. Amemiya and T. Seki, *Angew. Chem. Int. Ed.*, 2012, **51**, 5884-5888.

19. M. Sano, S. Nakamura, M. Hara, S. Nagano, Y. Shinohara, Y. Amemiya and T. Seki, *Macromolecules*, 2014, **47**, 7178-7186.

20. M. Sano, M. Hara, S. Nagano, Y. Shinohara, Y. Amemiya and T. Seki, *Macromolecules*, 2015. DOI: 10.1021/acs.macromol.5b00299.

21. K. Fukuhara, Y. Fujii, Y. Nagashima, M. Hara, S. Nagano and T. Seki, *Angew. Chem. Int. Ed.*, 2013, **52**, 5988-5991.

22. D. A. Shipp, J.-L. Wang and K. Matyjaszewski, *Macromolecules*, 1998, **31**, 8005-8008.

23. R. W. Richards and J. L. Thomason, *Macromolecules*, 1983, **16**, 982-992.

24. K. Y. Suh and H. H. Lee, *Macromolecules*, 1998, **31**, 3136-3138.

25. C. Osuji, P. J. Ferreira, G. Mao, C. K. Ober, J. B. Vander Sande and E. L. Thomas, *Macromolecules*, 2004, **37**, 9903-9908.

26. E. Verploegen, T. Zhang, Y. S. Jung, C. Ross and P. T. Hammond, *Nano Lett.*, 2008, **8**, 3434-3440.

27. A. M. Mayes and M. Olvera de la Cruz, *J. Chem. Phys.*, 1989, **91**, 7228-7235.

28. A. M. Mayes and M. O. de la Cruz, *J. Chem. Phys.*, **95**, 1991, 4670-4677.

29. V. Olszowka, M. Hund, V. Kuntermann, S. Scherdel, L. Tsarkova and A. Böker, *ACS Nano*, 2009, **3**, 1091-1096.

30. H. G. Schoberth, V. Olszowka, K. Schmidt and A. Boker, *Adv. Polym. Sci.*, 2010, **227**, 1-31.

Scheme and Figure Captions

Scheme 1. Chemical structures of polymers (a), and schematic illustration of photoinduced realignment process (b).

Fig. 1. Changes in *DR* (normalized) with time or light exposure dose for a series of $PBMA_m$-*b*-PAz_n diblock copolymers with different molecular masss (a), and comparisons of PBMA-*b*-PAz, PAz-*b*-PBMA-*b*-PAz triblock copolymer and PAz homopolymer. Symbols denote the data for $PBMA_{127}$-*b*-PAz_{76} (black circle), $PBMA_{102}$-*b*-PAz_{97} (red circle), $PBMA_{211}$-*b*-PAz_{145} (blue circle), PAz_{58}-*b*-$PBMA_{89}$-*b*-PAz_{58} (square) and PAz_{70} homopolymer (triangle).

Fig. 2. 2D GI-SAXS images and azimuthal 1D intensity profiles in the small and wide angle regions of initially LPL-aligned sample (left) and after successive LPL irradiation in the orthogonal direction (right). Parts a – c show data for diblock copolymer ($PBMA_{102}$-*b*-PAz_{97}) (a) triblock copolymer (PAz_{58}-*b*-$PBMA_{89}$-*b*-PAz_{58}) (b), and homopolymer (PAz_{70}).

Fig. 3. Scheme of experimental setup for GI-SAXS measurements (a), and examples for decaying (a) and enhancing (b) processes of X-ray scattering intensity from the smectic Az layer structure upon irradiation with successive (orthogonal) LPL. Triangles, circles, and square symbols denote data obtained with PAz_{70}, $PBMA_{102}$-*b*-PAz_{97}, and PAz_{58}-*b*-$PBMA_{89}$-*b*-PAz_{58}, respectively.

Fig. 4. T_{65} as a function of cylinder-to-cylinder distance of MPS (d) for decaying (a) and enhancing (b) processes of GI-SAXS scattering intensity due to the smectic Az layer structure. Filled circles and open squares denote data obtained with diblick and triblock copolymers, respectively. For the definition of T_{65}, see the text.

Fig. 5. POM images for films (250 nm thickness) of PBMA$_{127}$-*b*-PAz$_{76}$ (cylinder-to-cylinder distance, d = 29 nm) (a), PBMA$_{211}$-*b*-PAz$_{145}$ (d = 59 nm) (b), Az$_{58}$-*b*-PBMA$_{89}$-*b*-PAz$_{58}$ (d = 33 nm) (c), and PAz$_{70}$ (d) taken at the intermediate state where DR = 0.

Fig. 6. Combined representations of course profiles, changes in DR (normalized) taken from Fig. 2, and time courses of GI-SAXS intensity taken from Fig. 3 with exposure energy of LPL for diblock (PBMA$_{102}$-*b*-PAz$_{97}$) (a) and triblock (PAz$_{58}$-*b*-PBMA$_{89}$-*b*-PAz$_{58}$) (b) copolymers.

Fig. 7. Time course changes of GI-SAXS peak intensity due to MPS cylinder array with (open circle) and without (close square) light exposure (436 nm, 1 mW cm^{-2}) for the PBMA$_{127}$-*b*-PAz$_{76}$ film (a). In part b, T_{65}(decay) obtained by the GI-SAXS intensity decay due to the smectic Az layer structure was plotted against the cylinder to cylinder distance. Symbols are the same as used in Fig. 4.

a

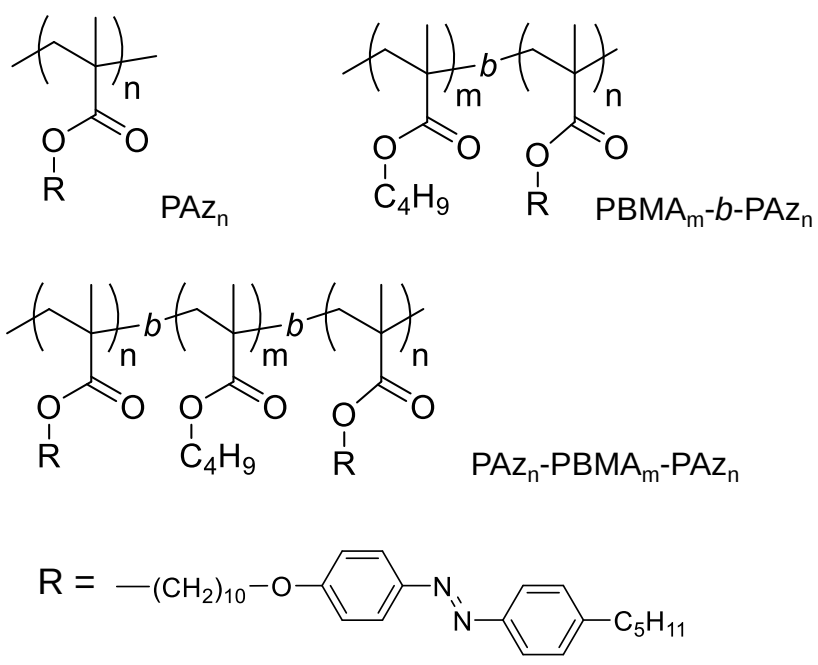

b

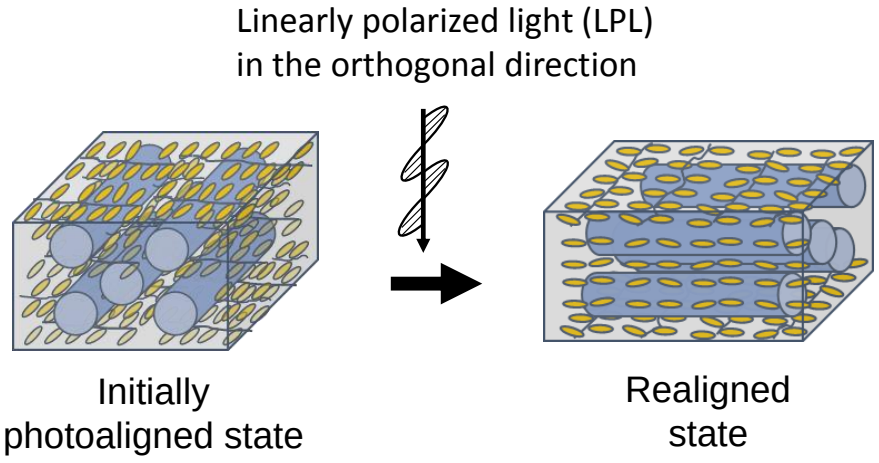

Scheme 1

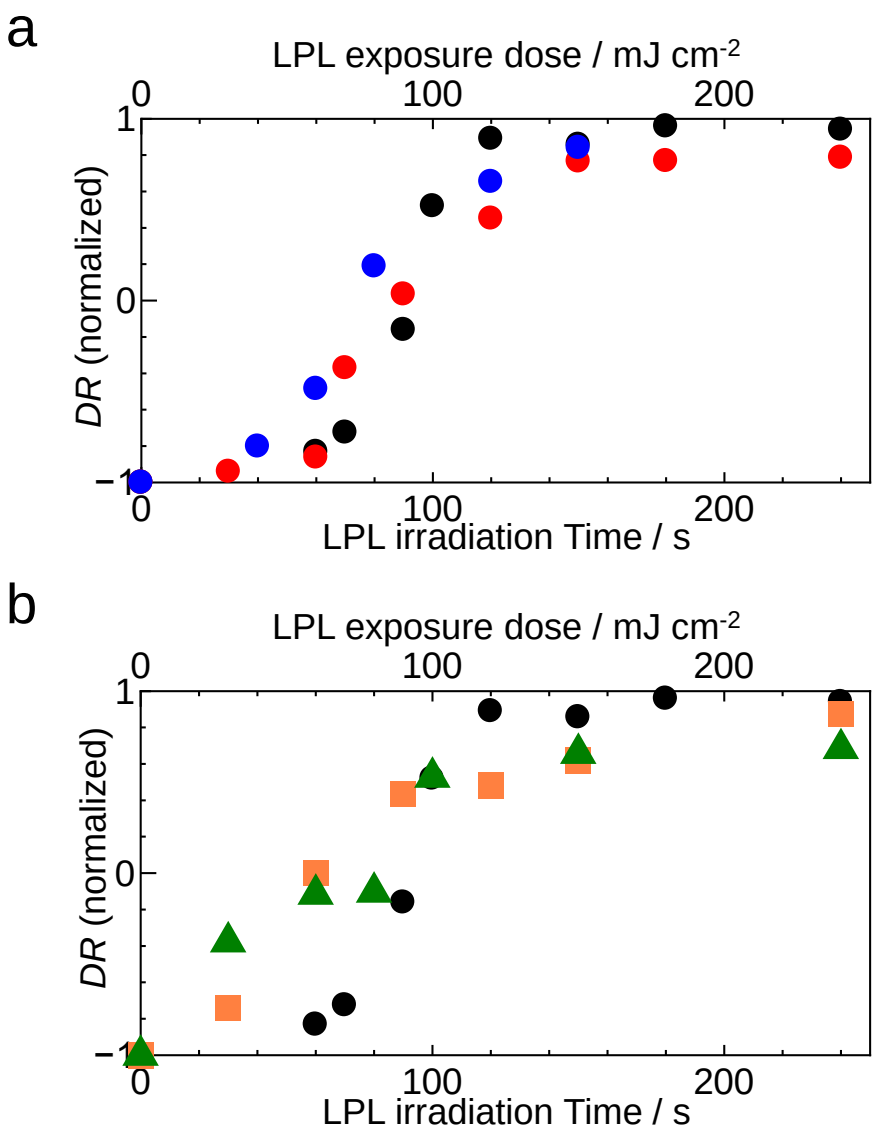

Fig. 1

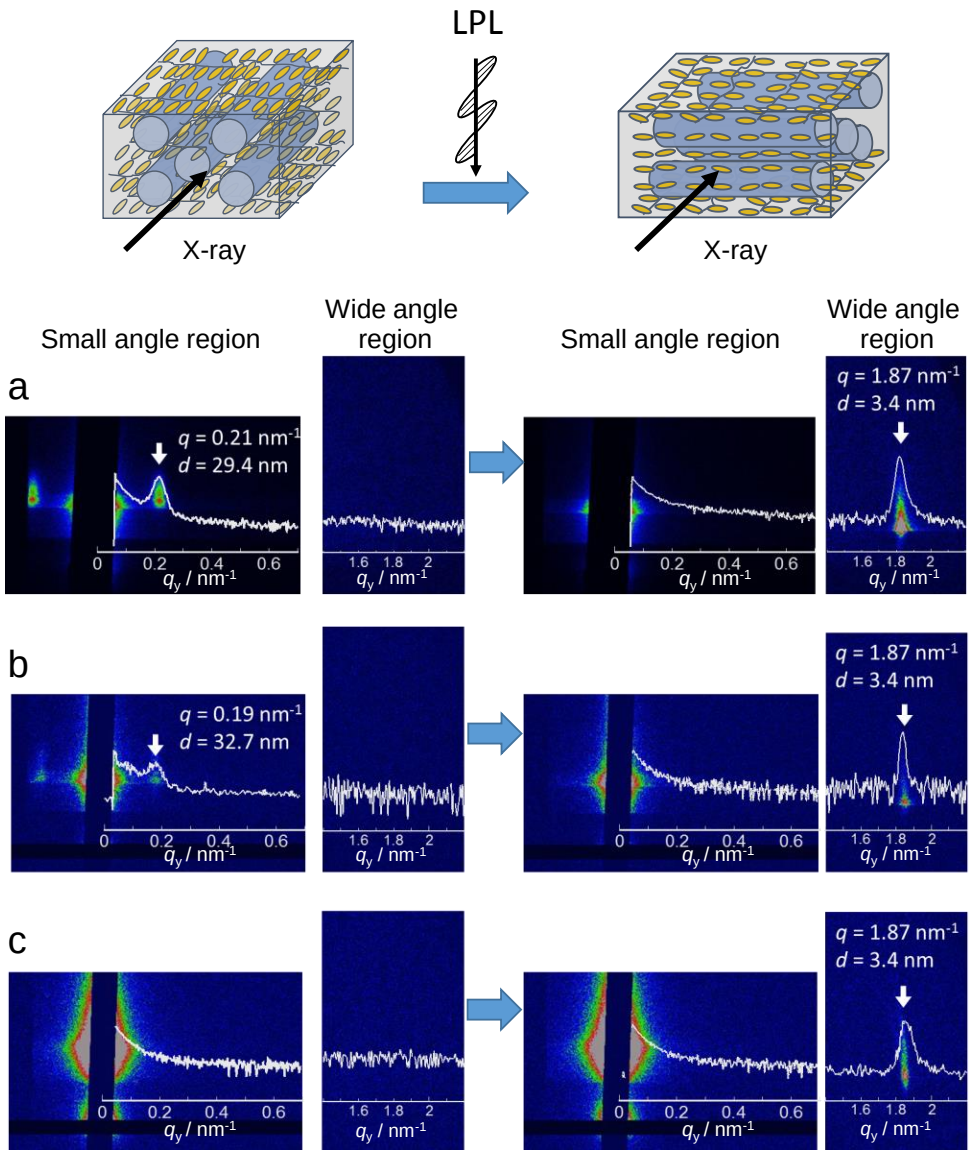

Fig. 2

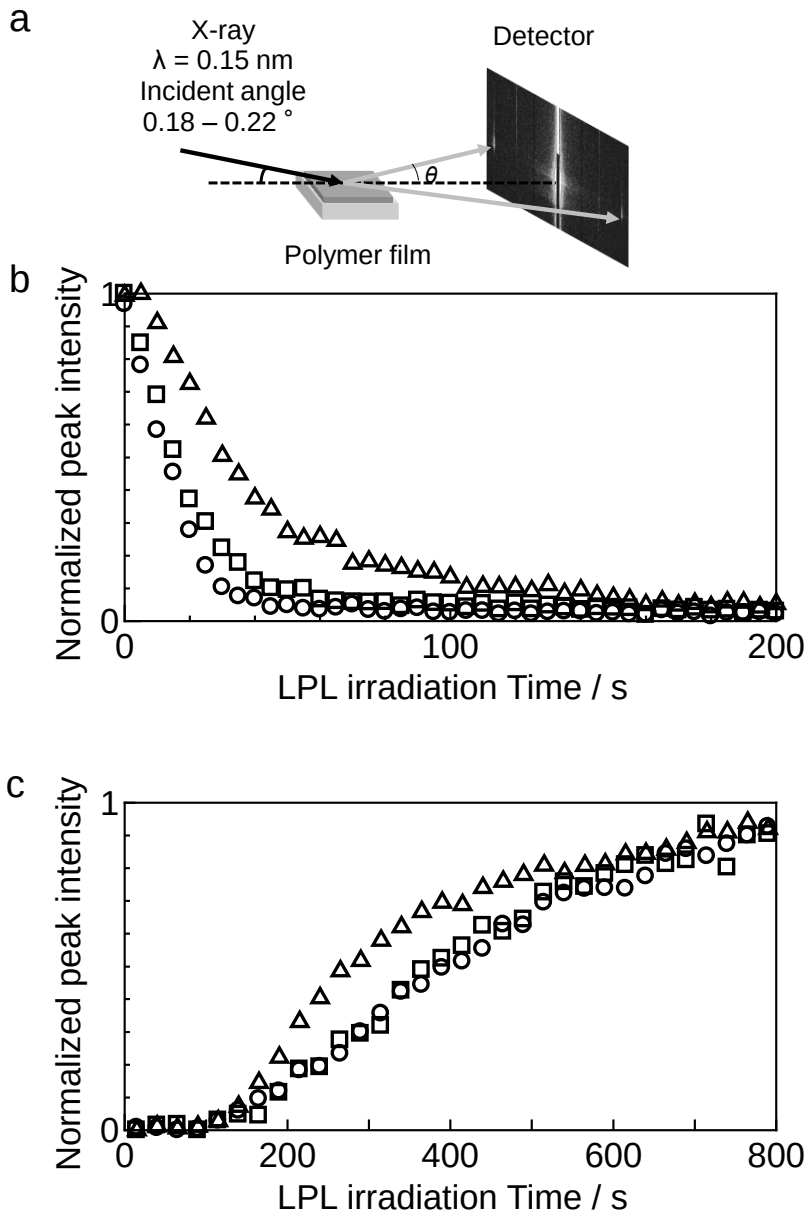

Fig. 3

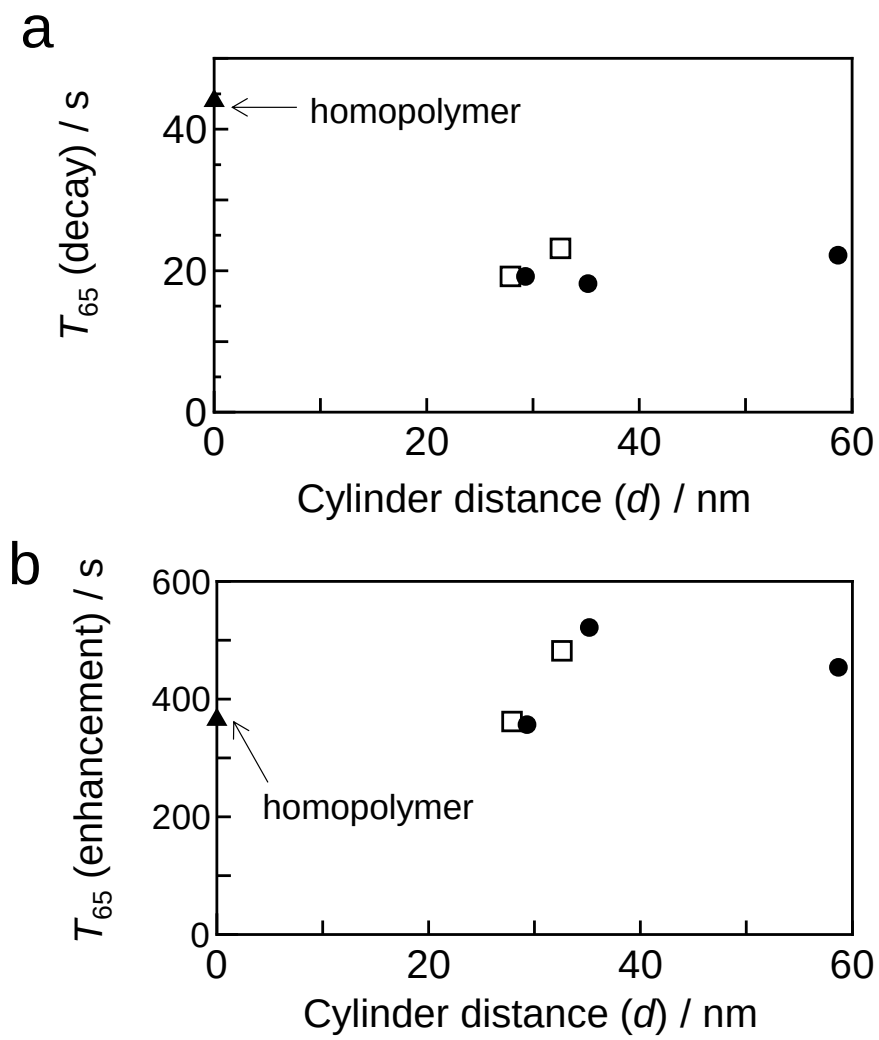

Fig. 4

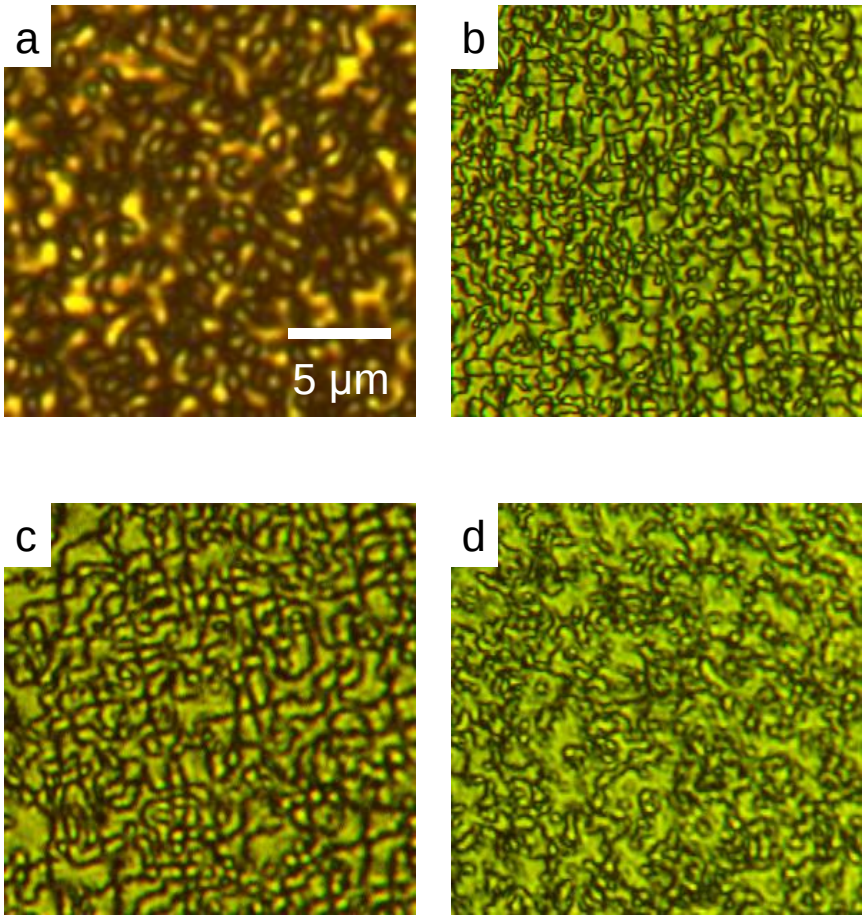

Fig. 5

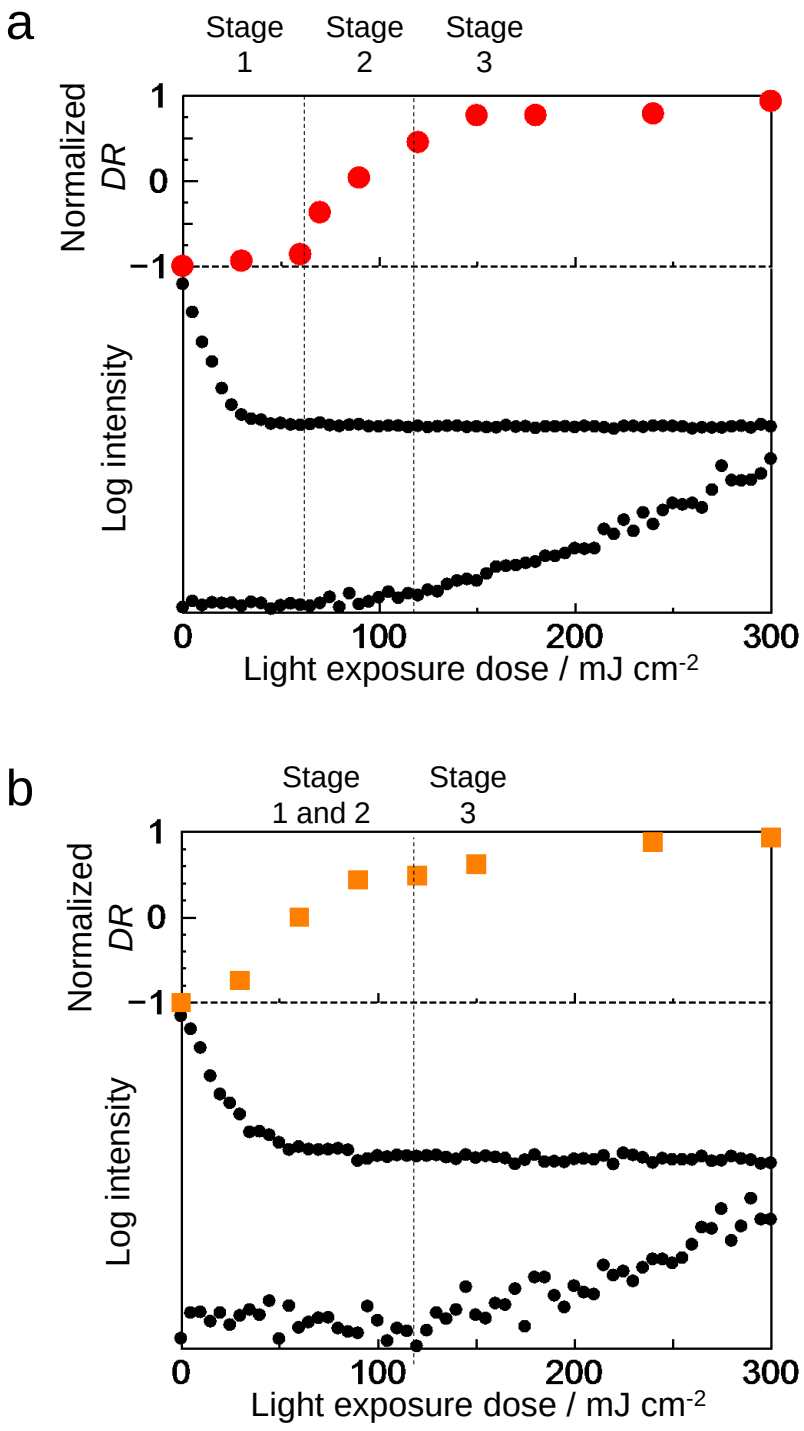

Fig. 6

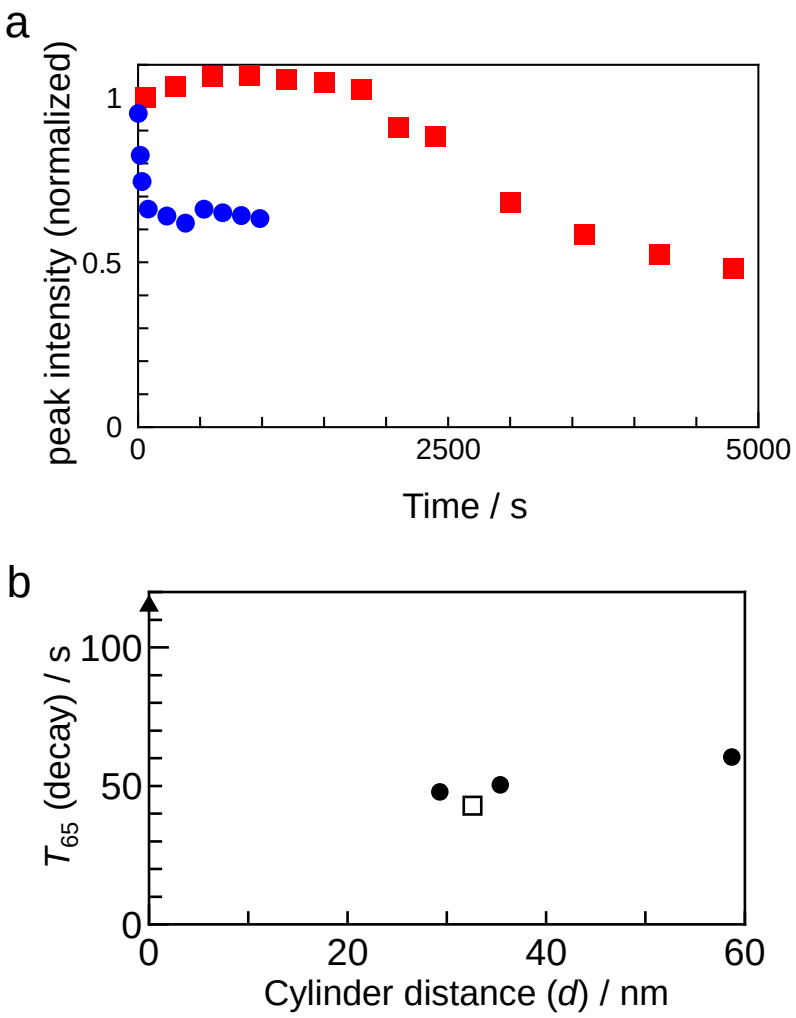

Fig. 7

Table of Contents

Dynamic photoinduced realignment processes in photoresponsive block copolymer films: Effects of chain length and block copolymer architecture

Masami Sano, Feng Shan, Mitsuo Hara, Shusaku Nagano, Yuya Shinohara, Yoshiyuki Amemiya, and Takahiro Seki

The feature of realignment process of microphase separated cylinder structure in azobenezene-containing liquid crystalline block copolymer films was significantly affected by the polymer architecture as revealed by in situ synchrotron GI-SAXS measurements.